The lipid type affects the *in vitro* digestibility and β-carotene bioaccessibility of liquid or solid lipid nanoparticles

Heloísa Helena de Abreu-Martins[b], María Artiga-Artigas[a], Roberta Hilsdorf Piccoli[b], Olga Martín-Belloso[a], Laura Salvia-Trujillo[a*]

[a]Department of Food Technology, University of Lleida – Agrotecnio Center, Av. Alcalde Rovira Roure 191, 25198. Lleida, Spain

[b]Department of Food Science, Federal University of Lavras, Av. Dr Sylvio Menicucci 1001, 37200000. Lavras, Brazil.

*Author to whom correspondence should be addressed

e-mail list:

Heloísa Helena de Abreu-Martins	heloisa_habreum@estudante.ufla.br
María Artiga-Artigas	maria.artiga@udl.cat
Roberta Hilsdorf Piccoli	rhpiccoli@dca.ufla.br
Olga Martín-Belloso	omartin@teca.udl.cat
Laura Salvia-Trujillo	lsalvia@tecal.udl.cat

Submitted to <Food Chemistry> on <July, 2019>

Running Title:

<Digestibility of solid lipid nanoparticles>

Keywords:

Solid lipid nanoparticles; oil type; β-carotene; lipid digestibility; bioaccessibility

Abstract

Solid lipid nanoparticles (SLNs) are emulsion-based carriers of lipophilic bioactive compounds. However, their digestibility may be affected by the solid lipid phase composition. Hence, the aim of this work was to study the *in vitro* lipolysis kinetics as well as the relationship between the lipid digestion, micelle fraction composition and β-carotene bioaccessibility of SLNs with different solid lipids, being blends of medium chain triglyceride (MCT) oil, glyceryl stearate (GS) or hydrogenated palm oil (HPO) as compared to liquid lipid nanoparticles (LLNs) with pure MCT. SLNs formulated with GS were fully digested, similarly to LLNs. However, HPO-containing SLNs presented slower lipolysis kinetics during the intestinal phase at increasing HPO concentration. Despite this, HPO-SLNs showed higher β-carotene bioaccessibility, which was related to the higher amount of monounstaturated free fatty acids in the micelle fraction. Thus, this work provides valuable insight for designing delivery systems of bioactive compounds with optimal functionality.

1 Introduction

In recent years, there has been an increasing interest on the design of emulsion-based delivery systems of lipophilic bioactive ingredients in food systems. In this regard, the fabrication of nanoemulsions as carriers of active compounds has arose as a strategy to enhance the functionality of health-related ingredients (Salvia-Trujillo, Soliva-Fortuny, Rojas-Grau, McClements, & Martin-Belloso, 2017). Nanoemulsions are dispersions of two immiscible liquids, typically oil-in-water, with a droplet diameter smaller than 200 nm (J. Rao & McClements, 2011). Nanoemulsions have shown a faster lipid digestibility kinetics under simulated gastrointestinal conditions in comparison with conventional emulsions with larger droplet sizes, which is attributed to their higher interfacial area able to interact with intestinal lipases (Salvia-Trujillo, Rojas-Graü, Soliva-Fortuny, & Martín-Belloso, 2013). This has been related with an enhancement of the functionality of lipophilic bioactive compounds, such as carotenoids. Carotenoids are hydrophobic micronutrients found in fruits and vegetables and their consumption has been associated with a reduced risk of cataract or cancer prevention (Rao & Rao, 2007). However, they are poorly solubilized in the intestinal juices due to their lipophilic nature, thus showing a very low bioaccessibility. The use of nanoemulsions as carriers of carotenoids has shown to enhance their bioaccessibility, which has been highly related to the oil droplet digestibility (Salvia-Trujillo et al., 2017). The higher the concentration of free fatty acids released from the lipid digestion, the higher the concentration of lipid species in the micellar fraction, and subsequently, the higher carotenoid micellarization capacity (Salvia-Trujillo et al., 2017). However, this relationship may be affected by other emulsion characteristics and the lipid composition such as the fatty acid chain length (Salvia-Trujillo, Qian, Martín-Belloso, & McClements, 2013) or their unsaturation degree (Verkempinck, Salvia-Trujillo, Moens,

Carrillo, et al., 2018), showing different carotenoid micellarization capacity and therefore bioaccessibility. Additionally, also the type of carotenoid species present different intrinsic bioaccessibility, which is related to their hydrophobicity, being β-carotene the one presenting the highest bioaccessibility (Palmero, Panozzo, Simatupang, Hendrickx, & Van Loey, 2014).

Moreover, carotenoids are often highly sensitive to suffer degradation due to the exposure to oxidative agents in the environment (Boon, McClements, Weiss, & Decker, 2010). Therefore, strategies are being sought in order to overcome their chemical instability. In this regard, solid lipid nanoparticles (SLNs), which are nanoemulsions yet consisting on a solid lipid core, have been reported to provide higher chemical stability of encapsulated lipophilic bioactive compounds in comparison with those formulated with liquid lipids (Muller, Mader, & Gohla, 2000; Nik, Langmaid, & Wright, 2012). This has been attributed to a reduced diffusion between the lipid core and the bulk aqueous phase (Salvia-Trujillo et al., 2019). However, depending on the crystallization state of the solid lipid core, an expulsion of the encapsulated bioactive compound may occur subsequently inducing a faster degradation (Weiss et al., 2008). In fact, certain solid fats may render tightly packed crystalline structures thus showing a faster degradation of carotenoids (Qian, Decker, Xiao, & McClements, 2013). In addition to this, differences have been observed in the lipid digestibility of emulsified solid lipids in comparison with liquid oils, by presenting a delayed lipolysis (Guo, Bellissimo, & Rousseau, 2017; Nik, Langmaid, & Wright, 2012; Salvia-Trujillo et al., 2019b). This behavior has being attributed to a hindered lipase adsorption onto lipid-water interfaces (Bonnaire et al., 2008), which might create opportunities towards a controlled lipid digestibility of such delivery systems. Nonetheless, most of recent research works dealing with the study of edible SLNs as delivery systems of bioactive compounds have

been conducted with purified solid lipids such as tripalmitin or tristearin among other triglycerides that are solid at room temperature (Mehnert & Mäder, 2001; Qian et al., 2013). However, the extrapolation of these studies to SLNs fabricated with commercially available solid fats is limited due to that solid fats are more complex in triglyceride composition and therefore they may present a different behavior during digestive conditions. Therefore, there is a need for a deeper understanding on the influence of the solid fat type and composition on the lipid digestibility kinetics and its relationship with the bioaccessibility of the encapsulated bioactive compounds.

Hence, the aim of this work was to study the fate during *in vitro* digestive conditions of liquid lipid nanoparticles (LLNs), also known as nanoemulsions, with medium chain tryglyceride oil (MCT) and SLNs formulated with lipid phases consisting on blends of MCT and two different solid lipid types, being glyceryl stearate (GS) or partially hydrogenated palm oil (HPO) at different concentrations as carriers of β-carotene. GS is a monoglyceride composed mainly of stearic acid (C18:0), which is typically used as surfactant in the food industry, while partially HPO is a triglyceride mainly consisting on palmitic (C16:0) and stearic acid (C18:0). For this purpose, the influence of the concentration of each solid fat on the *in vitro* lipid digestibility kinetics and the relationship with the β-carotene bioaccessibility was evaluated. Additionally, the micellar fraction composition was analyzed in order to identify the lipid species responsible for the β-carotene micellarization capacity.

2 Material and Methods

2.1 Materials

MCT oil (Mygliol® 812N) and GS (Imwitor® 491) with a purity of 99.9% and 96.7% (0.8% free glycerol and 95.9% monoglycerides), respectively, according to their certificate of analysis were purchased from IOI Oleochemical GmbH (Hamburg, Germany) and organic HPO containing ≤0.1 free fatty acids was acquired from Mystic Moments (Hants, UK). Tween 80, synthetic β-carotene (purity ≥ 93 %) and the rest of chemicals used in this study were purchased from Sigma-Aldrich, Inc. (St. Louis, MO, USA). Ethanol and hexane were from Fischer Scientific (Madrid, Spain). LLNs and SLNs were formulated with ultrapure water obtained from a Milli-Q filtration system (18.2 mΩ, Merck Millipore, Madrid, Spain).

2.2 Formation of liquid or solid lipid nanoparticles

LLNs with pure MCT or SLNs with different lipid phases consisting on blends of MCT and GS or HPO were formulated. GS or HPO were firstly melted by increasing the temperature at 60 ºC and subsequently were mixed with magnetic stirring at 500 rpm for 10 min with MCT at the same temperature. Specifically, the lipid phases containing GS were formulated with a 0.5, 1 or 5 % (*w/w*) of GS and the rest MCT, while those with HPO were blends of MCT:HPO at different ratios, being 50:50, 25:75 and 0:100. The selection of the concentration of GS and HPO, respectively, for the formulation of SLNs was done according to the minimum concentration that led to a solid lipid blend after being cooled down at 4 ºC for 1 hour, and the maximum concentration was set to the one that allowed the subsequent emulsification by microfluidization without risk of clogging. The concentration range tested for the two solid lipids was set according to the differences in their solidification behavior at room temperature and to avoid the

clogging risk of the high-pressure homogenization device during emulsification. The thermal properties of the lipid blends were characterized by differential scanning calorimetry (Mettler-Toledo 822e, Barcelona, Spain) from -20 to 80 ºC at 1 K/min (**supplementary material, Tables A and B**). Afterwards LLNs or SLNs were prepared by cold or hot high-pressure homogenization technique respectively, maintaining emulsions slightly above 60 ºC in order to avoid fat crystallization during the emulsification step in the case of the SLNs. Firstly, coarse emulsions were prepared by mixing the lipid phase at a 5 % (*w/w*), Tween 80 at a 2,5 % (*w/w*) as surfactant and the 92.5% of aqueous phase with a high-speed blender (Ultra-Turrax T25 homogenizer, IKA® Works, Inc. Wilmington, NC, USA) working at 7600 rpm for 3 min. The coarse emulsions were subsequently passed through a microfluidizer (MP-110 Microfluidics, MA, USA) at 70 MPa for 3 cycles. Afterwards, the temperature of LLNs or SLNs was reduced down to 4 ºC for 2 h in order to allow fat recrystallization.

2.3 *In vitro* digestion

The *in vitro* digestibility of LLNs and SLNs was conducted according to the INFOGEST international consensus (Minekus et al., 2014), consisting on a gastric and intestinal phase. Simulated gastric fluid solution (SGF) was consisted on a mixture of electrolytes [0.5 M KCl, 0.5 M KH_2PO_4, 1 M NaCl, 2 M NaCl, 0.15 M $MgCl_2(H_2O)$, 0.5 M $(NH_4)_2CO_3$] dissolved in 20 mL of milli-Q water. Then, 18.2 mL of SGF was acidified adding 1.8 mL of 0.02 M HCl, and used to dissolve the pepsin (8.8 mg/mL). Gastric digestion was performed by mixing 20 mL of LLNs or SLNPs with 20 mL of SGF solution. The mixture was incubated under subdued light conditions for 2 h at 37 °C and continuous agitation using an orbital shaker working at 100 rpm. Afterwards, a 30 mL-aliquot of the chyme was placed in a water bath at 37 °C. Subsequently, in order to simulate the small intestinal phase, 3.5 mL of bile salts (54 mg/mL) and 1.5 mL of

intestinal salts (10 mM of $CaCl_2$ and 160 mM of NaCl) were added to the sample, and the pH was adjusted to 7.0. Then, 2,5 mL of pancreatin (215 mg/mL) solution was added to the sample to initiate the lipid hydrolysis. The lipolysis reaction was monitored with a titration unit (pH-stat, Metrohm USA Inc., Riverview, FL, USA), which maintained the pH of the digest at 7. After this, digest samples were transferred into glass tubes and heat-shocked at 85 °C for 5 min in order to stop the lipolysis reaction and placed in an iced-water bath afterwards. The free fatty acid (FFA) release in percentage was calculated according to equation 1:

$$FFA\ (\%) = \frac{V_{NaOH} x\ C_{NaOH}\ x\ M_{oil}}{2\ x\ m_{oil}}\ x\ 100 \qquad \text{Equation (1)}$$

where V_{NaOH} is the NaOH volume needed to neutralize FFA released during the lipolysis reaction, C_{NaOH} is the Molar concentration of NaOH (0.25 M), M_{oil} is the molecular weight of the lipid phase (g/mol) and m_{oil} is the total oil weight in the 30-mL aliquot placed in the titration unit. The molecular weight of MCT oil, GS and HPO was 506, 1704 and 828 g/mol, respectively, and that of the blends was calculated taking into account the amount of each lipid component in the lipid phase.

2.4 Particle size and particle size distribution

The particle size and particle size distribution was measured by either dynamic or static light scattering technique using a Zetasizer Nano ZS or a Mastersizer 3000 (Malvern Instruments Ltd, Worcestershire, UK), respectively. For dynamic light scattering measurements sample was diluted 1:100 in MilliQ water and the particle size was reported as z-average (µm). For static light scattering measurements, sample was dispersed in a liquid dispersion unit and the particle size was reported as volume-weighted average ($d_{4,3}$).

2.5 ζ-potential

The ζ-potential (mV) was measured by phase-analysis light scattering (PALS) with a Zetasizer Nano ZS laser diffractometer (Malvern Instruments Ltd, Worcestershire, UK). Samples were prior diluted in ultrapure water using a dilution factor of 1:150 sample-to-solvent.

2.6 Microscopy

Phase contrast microscopy images of undiluted initial LLNs and SLNs and after being submitted to gastric and intestinal conditions were taken with an optical microscope (BX41, Olympus, Göttingen, Germany) equipped with UIS2 optical system. All images were processed using the instrument software (Olympus cellSense, Barcelona, Spain).

2.7 β-carotene bioaccessibility

The β-carotene bioaccessibility from LLNs and SLNs with different lipid phase composition was determined after the samples had been subjected to the prior described *in vitro* digestion procedure. An aliquot of the digest was ultracentrifuged (AVANTI J-25, Beckman Instruments Inc., Fullerton, CA, USA) at 15000 rpm for 40 min at a temperature of 8 °C. The supernatant, being the aqueous fraction containing the mixed micelles, was collected and was considered to be the micelle fraction in which the β-carotene is solubilized. The β-carotene quantification was conducted by the method reported by Liu et al. (2018), where a 0.5 mL-aliquot of the initial LLNs or SLNs and the micellar fraction was mixed with 2 mL of ethanol and 3 mL of hexane and vortexed for 10 s. Afterwards, the upper hexane phase containing the β-carotene was transferred to a test tube and the extraction was repeated two times until the ethanol lower layer was clear. The hexane fraction was analyzed spectrophotometrically (CECIL CE 2021; Cecil Instruments Ltd, Cambridge, UK) at 450 nm. The concentration of β-carotene extracted from a sample was determined from a calibration curve of absorbance versus β-carotene

concentration in hexane. The bioaccessibility was then calculated using the following equation:

$$BA = \frac{C_{micelle}}{C_{initial}} \times 100 \qquad \text{Equation (2)}$$

where $C_{micelle}$ and $C_{initial}$ are the β-carotene concentration in the micellar fraction and the initial LLNs or SLNs, respectively.

2.8 Micellar fraction analysis

The micelle fraction of the digested LLNs and SLNs formulated with different lipid phases was characterized in terms of their concentration of lipid digestion products. A 1-mL aliquot of the micelle fraction was mixed with 2 mL of ethanol, 3 mL of diethylether:heptane (1:1) and 0.2 mL of sulphuric acid (2.5 M), vortexed for 2 min and further stirred at 200 rpm during 30 min. Afterwards, the top layer was collected in a 5 mL volumetric flask containing 100 mg of Na_2SO_4 (anhydrous). The bottom layer was mixed with 1 mL of diethylether:heptane (1:1) and the process was repeated and stirred for 15 min. The organic layer was added to the previous one and the volume was brought up to 5 mL. The lipid extract was kept at −40 °C until analysis. The analysis and relative quantification of the lipid digestion products was carried out with a 6890-5973 Gas Chromatograph-Mass Spectrometer (GC-MS) (Agilent Technologies, USA) based on a method previously proposed with some modifications (Verrijssen et al., 2016). In the GC with a capillary column ZEBRON ZB-1HT (15 m x 0.32 mm x 0.25 µm) (Inferno™, Phenomenex, Madrid, Spain), 0.5 µL sample was injected on-column. The oven temperature started at 80 °C and increased to 400 °C through a first ramp of 6 °C/min up to 280ºC followed by a second one of 30ºC/min until 380ºC (1 min). An MS-system (Agilent Technologies, 5973 Inert Mass Selective Detector, Diegem, Belgium, U.S.A) was used to detect the compounds. Nist 11 Mass spectral library was used as

227 standard reference database for the identification of FFAs and MAGs (FarHawk
228 Marketing Services, U.S.A). The quantification of FFAs and MAGs was carried out by
229 comparison with standard curves of decanoic acid (C10:0), dodecanoic acid (C12:0),
230 myristic acid (C14:0), palmitic acid (C16:0), stearic acid (C18:0) and oleic acid (C18:1)
231 for FFAs and 1-octanoyl-rac-glycerol (MAG-C8:0), 1-decanoyl-rac-glycerol (MAG-
232 C10:0), 2-palmitoylglicerol (MAG-C16:0), 1-oleoyl-rac-glycerol (MAG-C18:1) for
233 MAGs.

234 ## 2.9 Lipolysis kinetics

235 The kinetics of the lipolysis reaction at early time moments (35 min) of the *in vitro*
236 small intestinal phase of LLNs or SLNs formulated with GS or HPO at different
237 concentrations was evaluated by fitting a logistic model consisting of 3 estimated
238 parameters (Equation 3) to FFA release experimental data.

239 $$FFA(t) = \frac{b}{1+e^{-k(time-a)}}$$ Equation (3)

240

241 where *FFA(t)* is the free fatty acid release (%) during small intestinal phase time *(t)*, *a* is
242 the inflexion point of the curve (min); *b* is the asymptotic value of the curve (%) when
243 small intestinal phase time (*t*) is ∞; and *k* is the reaction rate constant (min^{-1}).

244 Estimated parameters were determined by non-linear regression using the JMP Pro 14
245 statistical software (SAS Institute Inc.). The fit of the model was assessed by calculating
246 R^2 and visually analyzing the residue plots. Significant differences between the
247 estimated parameters of different samples were determined by calculating the
248 confidence intervals (95%).

2.10 Statistical analysis

All experiments were performed in duplicate, using at least two measurements of each determination. An analysis of variance was carried out and the Student's t test was run to determine significant differences at a 5% significance level ($p < 0.05$) with statistical software JMP Pro 14 (SAS Institute Inc.).

3 Results and discussion

The influence of the lipid phase state of LLNs or SLNs formulated with GS or HPO during *in vitro* digestive conditions was studied in terms of (*i*) their colloidal stability through their particle size, particle size distribution, microstructure and ζ-potential; (*ii*) their lipoplysis kinetics during small intestinal phase by determining the FFA release; (*iii*) the β-carotene bioaccessibility after the *in vitro* digestive conditions and (*iv*) the composition of the micellar fraction in terms of lipid species in order to elucidate the relationship between the lipolysis kinetics, the β-carotene bioaccessibility and the micellar fraction composition.

3.1 Colloidal stability during *in vitro* digestion

The stability of initial LLNs or SLNs containing GS or HPO at different ratios after being submitted to simulated gastric and small intestinal phases was studied.

Particle size, particle size distribution and microstructure

The initial particle size of LLNs containing pure MCT was 0.110 ± 0.013 µm while SLNs formulated with MCT and GS presented slightly yet significantly smaller particle sizes, with values of 0.987 ± 0.001 µm in SLNs formulated with 1 % GS in the lipid phase (**Figure 1A**). In fact, GS is a monoglyceride with interfacial activity, thus contributing to some extent to the particle size reduction during emulsification. Despite this, no significant differences were observed after increasing the concentration of GS in

the lipid phase of SLN, suggesting that a concentration of 0.5% is enough to evidence its emulsifying capacity, without presenting a significant reduction in the particle size of SLN when used at higher concentrations. However, SLNs formulated with HPO presented a significantly higher initial droplet size (0.136 ± 0.001 μm) in comparison with pure MCT LLNs (**Figure 1B**), which may be attributed to the higher viscosity of solid fats, such as HPO, in comparison with oils with medium chain triglycerides. In this regard, microscopy images evidenced a larger droplet size in those SLNs formulated with a 25:75 MCT:HPO ratio and pure HPO (**supplementary material, Figure D**). Initial LLNs or SLNs formulated with either GS or HPO presented narrow particle size distribution (**Figure 2A, D**) and microscopy images showed homogeneous dispersion of lipid droplets (**supplementary material, Figure C and D**).

On the one hand, after simulated gastric conditions, the particle size of LLNs with MCT or SLNs with GS or HPO remained stable (**Figure 1A, B**). In fact, it has been previously reported that Tween 80 is a non-ionic surfactant, which is not sensitive to pH changes in the gastric phase (pH 3), thus showing higher stability of emulsion-based systems in the stomach in comparison with other emulsifiers (Verkempinck, Salvia-Trujillo, Moens, Charleer, et al., 2018). This was confirmed by the results of particle size distribution (**Figure 2B, E**) and microscopy images (**supplementary material, Figure C and D**), which showed the same results than initial MCT LLNs and SLNs.

Regarding the end of the small intestinal phase, a large increase in the particle size of MCT LLNs and SLNs was observed. In the case of MCT LLNs, the surface-weight (d_{32}) average particle diameter was 91 ± 5 μm, while it was smaller in those SLNs containing GS. Actually, significantly smaller particle size of the digest was observed as increasing the GS concentration in the SLN formulation. The d_{32} values for SLNs containing 0.5, 1 or 5 % (*w/w*) of GS in the lipid phase after being submitted to small

intestine conditions were 17 ± 3, 11 ± 2 and 7 ± 1 µm, respectively. Despite that the particle size distribution presented multimodal curves after intestinal conditions (**Figure 2C**), it was observed that LLNs with MCT presented a particle size distribution with a main intensity peak of large particles around 100 µm, while the particle size distribution of SLN presented intensity peaks of smaller particles. This suggests that, stearic acid released after lipolysis of GS may contribute to some extent to the emulsification of lipid species after the lipid hydrolysis. With regards SLN formulated with HPO, their particle size increase after small intestine conditions (**Figure 1F**) was less pronounced in comparison with those formulate with GS. The d_{32} values of SLNs at the end of the intestinal phase ranged between 0.69 ± 0.04 and 1.43 ± 0.36 µm, with intensity peaks in the particle size distribution below 10 µm, which might be attributed to the presence of undigested lipid particles from the SLNs containing HPO Additionally, microscopy images (**supplementary material, Figure C**) showed the presence of fibrous-like particles in those samples formulated with GS, which might be attributed to the crystallization FFA released, such as stearic acid, due to the decrease of temperature during the microscopy examination. Oppositely, HPO-containing SLNs presented smaller undigested solid lipid particles (**supplementary material, Figure D**).

ζ-potential

The particle electrical charge (ζ-potential) of LLNs with MCT and SLNs formulated with GS or HPO at different concentrations before and after being subjected to simulated gastric and small intestinal phases is presented in **Figure 3**. In this context, the ζ-potential of lipid particles might contribute in explaining differences in the stability during digestion and lipolysis degree. Initially, LLNs and SLNs showed negatively charged interfaces, with ζ-potential values ranging between -25.9 and -28.8 mV, without significant differences between them (**Figure 3**). In fact, the surfactant

used in this study (Tween 80) is a non-ionic emulsifier that has shown to present negative charge in emulsions and nanoemulsions at certain pH conditions (Salvia-Trujillo, Qian, Martín-Belloso, & McClements, 2013). After gastric conditions, both LLNs and SNLs formulated with GS or HPO exhibited a drastic decrease in the particle electrical charge, being less negatively charged, with values between -6.7 and -10.4 mV (**Figure 3**). This decrease in the ζ-potential after gastric conditions might be due to the lower pH (3) at the stomach phase, thus reducing the ionization degree of negatively charged groups. Nonetheless, after small intestinal conditions, the ζ-potential of the digested MCT LLNs and SLNs with GS and HPO at different concentrations decreased, observing differences between SLNs formulated with GS and HPO. On the one hand, LLNs and SLNs formulated with GS presented similar ζ-potential values after small intestinal conditions, with values ranging between -29.9 and -34.1 mV, without significant differences among SLNs with different GS concentrations (**Figure 3**). On the other hand, the ζ-potential of SLNs formulated with HPO was significantly more negative after small intestinal phase at increasing HPO concentration in the lipid phase (**Figure 3**). In this sense, the ζ-potential of MCT LLNs was -30.3 mV after small intestinal conditions, and it was -48.4, -51.6 and -52.5 mV in SLNs containing HPO at increasing concentrations being 50, 75 and 100 % HPO, respectively (**Figure 3**). It has been reported that the negative charge of digested emulsion-based systems after small intestinal phase can be attributed to the presence of anionic free fatty acids and other lipid digestion products from lipid hydrolysis (Singh, Ye, & Horne, 2009). However, our results show that SLNs formulated with increasing HPO concentration in the lipid phase, which had a more negative ζ-potential, where those that showed a lower lipid digestibility and therefore a lower FFA release (section 3.2). Therefore, this suggests that not only the concentration of lipid species released at the end of the intestinal phase

348 determines the charge of the digested samples, but also the FFA chain length plays a
349 key role on the charge of the digest. In this regard, it has been reported that the negative
350 charge of digested samples decreases at increasing the chain length of the released FFA
351 (Salvia-Trujillo et al., 2013). In fact, HPO mainly contains long chain fatty acids while
352 MCT contains medium chain fatty acids, thus explaining the differences in ζ-potential
353 after small intestinal conditions.

354 ## 3.2 Lipolysis kinetics during *in vitro* small intestinal phase

355 The lipolysis reaction was monitored during the *in vitro* small intestinal phase through
356 the FFA release (%) in order to determine differences between the behavior during lipid
357 digestion of LLNs and SLNs formulated with different concentration of GS or HPO
358 hence different solidification degrees (**Figure 4**).

359 For all the studied LLNs and SLNs, the lipid digestion reaction followed a sigmoidal-
360 shape curve, with a start of the lipolysis reaction immediately at the beginning of the
361 intestinal phase and subsequently followed by an exponential increase in the FFA
362 release at digestion time moments below 20 min. After this point, a steady-state zone
363 was reached, with a residual increase of the FFA until the end of the intestinal phase.
364 Nonetheless, both the lipid digestion kinetics at the beginning of the intestinal phase and
365 end-point values of FFA release were highly dependent on the lipid phase formulation,
366 with significant differences between LLNs and SLNs. Additionally, differences could
367 be established between the lipolysis kinetics of GS and HPO-containing SLNs.

368 On the one hand, MCT LLNs and the GS-containing SLNs presented similar lipid
369 digestion kinetics regardless the concentration of GS in the lipid blend (**Figure 4A**). In
370 fact, they presented similar rate constants (*k*-values) with values ranging between 0.328
371 and 0.351 (**Table A, supplementary material**). Therefore, this evidences that the

solidification of the lipid phase by adding GS to MCT does not affect their lipid digestibility kinetics. Nevertheless, at increasing GS concentration in the lipid phase, SLNs reached slightly higher FFA values at the curve asymptote (**Figure 4A, Table A, supplementary material**), which lead to significantly higher values of FFA release at the end of the intestinal phase (**Figure 4C**). For instance, MCT LLNs led to FFA release asymptotic values of 86.34 ± 0.96 %, while SLNs with 5 % (*w/w*) GS led to 98.37 ± 1.09 % FFA release. This might be due to the direct hydrolysis of stearic acid in the GS molecule, thus contributing to the overall lipid digestibility (Levy, Goldstein, Freier, & Shafrir, 1981). In fact, from triacylglycerols (TAG) hydrolysis, FFA and monoacylglycerols (MAG) are released. Pancreatic lipases present 1,3-n stereospecificity during TAG hydrolysis thus 2-n MAG normally remain undigested. Therefore, this suggests that GS may contain stearic acid in the 1- or 3-n positions, since it is hydrolyzed during small intestinal digestion of SLNs formulated with GS, accounting for the overall FFA release values.

On the contrary, the lipid digestibility kinetics and extent during the small intestinal phase of SLNs containing HPO was highly dependent on the concentration of HPO in the formulation of the lipid phase (**Figure 4B, D**). At early time moments of the small intestinal phase, there was a significant delay in the initiation of the lipolysis reaction at increasing concentrations of HPO, observing the slowest lipid digestion kinetics in SLNs formulated with 100% HPO as lipid phase (**Figure 4B**). This was evidenced by the estimated kinetic parameters of the sigmoidal equation (Eq. 3) used to model the FFA release data (**Table B, Supplementary material**). In fact, there was a significant increase in the *k*-values of those SLNs with MCT:HPO 50:50 or 25:75, being 0.476 and 0.460, in comparison with MCT LLNs, with a *k*- value of 0.351. Conversely, the asymptotic estimated parameter of SLNs formulated with 100% HPO evidenced that

there was a significantly lower FFA release in comparison SLNs with lower HPO content, reaching to values of 56.92 ± 2.55 % after 35 min of small intestinal phase, while it was 86.34 ± 0.96 % in MCT LLNs. This trend was maintained until the end of the small intestinal phase, where a lower lipid hydrolysis was observed in SLNs formulated at increasing concentration of HPO after 2 hours of intestinal conditions. In this regard, at the end of the intestinal phase, SLNs with 100% HPO presented 62 % FFA release, while MCT LLNs were fully digested, with a 100 % FFA release (**Figure 4C**).

The results of the current work evidence that lipid digestion kinetics is highly related to the specific crystalline state of the particular solid fats used as dispersed phase of SLNs. In fact, this might be attributed to the higher melting temperatures of HPO-containing SLNs in comparison with GS-containing SLNs, as observed in the DSC profiles of their respective lipid phases (**Supplementary material, Figures A and B**). Besides this, also the chain length of the fatty acids composing the triacylglycerol profile of the fats used in this work might contribute in explaining the differences observed. In fact, it is known that medium chain oils, such as MCT, present a faster and higher FFA release than long chain fatty acids in fats such as those present in HPO (Salvia-Trujillo et al., 2013), being attributed to that medium chain fatty acids are able to migrate more rapidly to the aqueous phase while long chain fatty acids tend to accumulate at the oil-water interface thus presenting a slower digestibility. Similarly to our findings, Guo et al. (2018) observed no significant differences between the lipid digestibility kinetics of emulsions stabilized with glyceryl monooleate or glyceryl monostearate, as liquid or solid emulsifiers, respectively. Moreover, other authors have reported that GS digestibility may not be concentration dependent, showing fast lipid digestibility regardless of the GS concentration in the lipid phase (Wang et al., 2017). Therefore, this suggests that

factors other than the lipid state may determine lipid digestibility of SLNs. In this context, Witzleb et al. (2012) observed that despite that both glyceryl monostearate and glyceryl tripalmitate are solid lipids, the former presented a much higher digestibility in comparison with glyceryl tripalmitate. Similarly, other authors have reported a much lower lipid digestibility in solid triacylglycerols such as tripalmitin, hydrogenated soy oil or cocoa butter in comparison with liquid dispersed phases (Bonnaire et al., 2008; Guo et al., 2017; Hart, Lin, Thilakarathna, & Wright, 2018). These differences in the lipid digestion behavior between solid monoacylglycerides and tryglycerides may be attributed to (*i*) the higher solubility of glyceryl monostearate in comparison with triacylglycerols thus being more accessible by pancreatic lipases and to (*ii*) the preference of intestinal lipase for MAG molecules such as glyceryl monostearate in comparison with TAGs.

3.3 β-carotene bioaccessibility after *in vitro* digestion

The concentration of β-carotene in the micelle fraction was determined and related to the initial concentration in LLNs and SLNs, thus accounting for the percentage of β-carotene that was incorporated into mixed micelles, being referred to as β-carotene bioaccessibility (**Figure 5A, B**). Additionally, the final amount of FFA released (%) at the end of the intestinal phase (120 min) was plotted in order to relate the β-carotene bioaccessibility with the lipid hydrolysis degree.

On the one hand, the β-carotene bioaccessibility of LLNs or GS-SLNs and their respective lipid digestion extent at the end of the intestinal phase were not positively correlated. In this regard, despite that the FFA release increased at increasing the GS concentration in the lipid blend, which was attributed to the digestion of GS

monoglyceride, the β-carotene bioaccessibility did not increase. In this sense, the β-carotene bioaccessibility was 28.1 ± 2.1 % in MCT LLNs and was practically similar or even slightly lower in the case of SLNs containing GS in the lipid phase (**Figure 5A**), being 25.8 ± 0.4, 22.6 ± 0.9 and 26.7 ± 0.4 % for SLNs with 0.5, 1 and 5% (*w/w*) GS, respectively. Nevertheless, the opposite behavior was observed in SLNs containing HPO in the lipid phase (**Figure 5B**). The lipolysis extent of the HPO-containing SLNs decreased at increasing the HPO concentration the lipid blend, yet the β-carotene bioaccessibility significantly increased. In this regard, the lipid digestion was decreased at the end of the intestinal phase from 106 ± 3 % in the MCT LLNs to 62 ± 2 % in the SLN formulated with pure HPO as lipid phase, while the β-carotene bioaccessibility increased from 28.1 ± 2.1 % up to 35.7 ± 1.4 %, respectively. Our results are in controversy with the generally accepted statement that a higher the concentration of lipid species in the digest might be positively correlated with an increase in the mixed micelles micellarization capacity of lipophilic bioactive compounds such as carotenoids (Singh et al., 2009). In this context, our results evidence that not only the degree of lipolysis during digestion, but also the type of micellarized lipid species might determine their β-carotene solubilization capacity as discussed in the following section.

3.4 Micellar fraction composition

The micelle fraction composition was characterized in terms of the concentration of FFA and MAGs after small intestinal conditions in order to identify those lipid species that are micellarized after being hydrolyzed (**Figure 6**) and that might be responsible for the β-carotene bioaccessibility.

On the one hand, the micelle fraction of LLNs and SLNs containing a blend of MCT and GS after being digested was composed mainly of caprylic (C8:0) and capric (C10:0) acids (**Figure 6A**), which are the main medium chain fatty acids present in MCT oil. In this regard, the concentration of caprylic and capric acids in the micelle fraction of the MCT LLNs was 154 ± 2 and 122 ± 2 mg/mL of micellar fraction, respectively. At increasing the concentration of GS in the lipid blend of SLNs, the concentration of long chain FFA in the micelle fraction increased, detecting the presence of stearic (C18:0) and oleic (C18:1) FFA, in expense of the concentration of medium chain fatty acids (C8:0 and C10:0), which decreased. The concentration of stearic FFA in the micelle fraction of SLNs had increasing values of 3.4 ± 0.3, 6.5 ± 1.2 and 8.6 ± 0.7 mg/mL at increasing the concentration of GS in the lipid blend. Additionally, the concentration of oleic acid ranged between 4.4 ± 0.9 and 5.8 ± 1.6 mg/mL of micelle fraction, regardless the concentration of GS in the lipid blend. A residual amount of palmitic FFA (C16:0) was detected in MCT LLNs and SLNs containing GS, with concentrations ranging between 1.02 ± 0.5 and 1.55 ± 0.8 mg/mL of micelle fraction. Furthermore, the presence of monocaprylin (MAG-C8:0) and monocaprilate (MAG-C10:0) was detected in SLNs containing 0.5 or 1 % (*w/w*) GS (**Figure 6B**). This results are in agreement with the lipid digestion kinetics results of the present work (**Figure 4A, C**), where a higher amount of FFA release was found, being attributed to the hydrolysis of the stearic acid of GS molecule. In fact, the absence of GS as monoglyceride form in the micelle fraction and the presence of stearic FFA instead support these results. However, the higher concentration of long chain fatty acids in the micelle fraction of SLNs with GS was not positively correlated with the β-carotene bioaccessibility results (**Figure 5A**), presenting a similar or even lower β-carotene bioaccessibility at the end of the intestinal phase. These findings are in controversy with previous reports evidencing that long

chain FFA may lead to a higher solubilization capacity of lipid species such as carotenoids (Salvia-Trujillo et al., 2013), being postulated to that long chain fatty acids may form larger mixed micelles, thus being able to better accommodate carotenoids in their inner core. Nevertheless, molecular characteristics other than the chain length might be involved in determining the mixed micelles solubilization capacity of lipophilic bioactive compounds.

On the other hand, the micelle fraction of SLNs formulated with a blend of MCT:HPO as lipid phase presented a higher concentration of long chain FFA (**Figure 5C**), being higher than that observed for SLNs containing GS (**Figure 5A**). In fact, the concentration of medium chain FFA such as caprylic and capric acids decreased, from values above 120 mg/mL in the micelle fraction of the MCT LLNs down to values below 60 mg/mL in the SLNs with MCT:HPO 50:50. At the same time, the concentration of long chain FFA, such as palmitic, stearic and oleic increased. For instance, the concentration of oleic FFA increased up to 16.5 ± 1.4, 31.7 ± 2.1 and 55.2 ± 3.3 mg/mL in the micelle fraction of SLNs containing MCT:HPO 50:50, 25:75 and 0:100, respectively. Additionally, significant amounts of MAGs with long chain fatty acid esters were found in the micelle fraction of HPO-containing SLNs (**Figure 6D**). In this regard, monopalmitin and monolein were found in concentrations around 2.8 ± 0.1 and 2.0 ± 0.1 mg/mL respectively, regardless the HPO concentration in the lipid blend. These results support that monounsaturated long chain fatty acids, such as oleic acid, confer a higher solubilization capacity to mixed micelles, since despite that the lipid digestion in terms of FFA release of the HPO-containing SLNs was much lower than MCT LLNs and GS-containing SLNs, they presented a higher β-carotene bioaccessibility (**Figure 5B**). In fact, oleic acid concentration in the micelle fraction increased with increasing the HPO concentration in the lipid blend, which was the only

lipid species positively correlated with the β-carotene bioaccessibility (data not shown). In agreement to this, other authors have reported that the fatty acid saturation degree might determine the micellarization capacity of mixed micelles, since monounsaturated FFA were related to a higher carotenoid bioaccessibility in comparison with polyunsaturated FFA (Verkempinck, Salvia-Trujillo, Moens, Carrillo, et al., 2018). Moreover, differences have been reported in the lipid digestion preference of intestinal lipases, being digested first the unsaturated fatty acids followed by monounsaturated and finally polyunsaturated fatty acids (Pascoviche, Goldstein, Fishman, & Lesmes, 2019). In this context, our results evidence that monounsaturated long chain FFA, such as oleic acid, might contribute in a higher extent compared to saturated long chain FFA such as palmitic acid, to the micellarization of β-carotene.

4 Conclusions

Results of the present research contribute to understanding the role of the lipid type and state on the colloidal stability and lipid digestion kinetics of solid lipid nanoparticles (SLNs) as carriers of lipophilic bioactive ingredients and the relationship between the micelle fraction composition and their bioaccessibility. In this regard, the lipid hydrolysis might be determined not only by the crystallization state of the lipid used for the formulation of SLNs but also by the chain length of the lipid type. The solidification of lipid phase consisting on a medium chain triglyceride oil (MCT) with a monoglyceride molecule such as glyceryl stearate (GS) does not affect the lipolysis reaction of SLNs during small intestine conditions whereas hydrogenated palm oil (HPO), which is mainly composed of long chain fatty acids, significantly slows down the lipid hydrolysis kinetics and diminishes its extent, which may be attributed to the

type of fat crystals formed with HPO-containing SLNs, hindering the adsorption of intestinal lipases at the oil-water interface. Additionally, it was evidenced that the β-carotene bioaccessibility and therefore the solubilization capacity of mixed micelles is not determined by the concentration of lipid digestion products in the micelle fraction but by the type of lipid species. Namely, the presence of monounsaturated long chain fatty acids, such as oleic acid, and long chain monoacylglycerols in the micelle fraction contribute in enhancing the β-carotene bioaccessibility. Hence, this work provides novel insights on the behavior of SLNs under digestion conditions and the possibility to modulate the formulation the solid lipid phase for a targeted lipid digestibility with optimal bioaccessibility of encapsulated lipophilic bioactive compounds.

Acknowledgements

This study was funded by the Ministry of Economy, Industry and Competitiveness (MINECO/FEDER, UE) throughout projects RTI2018-094268-B-C21 and AGL2015-65975-R. Heloísa Martins thanks for the scholarship financed by "Coordenação de Aperfeiçoamento de Pessoal de Nível Superior" (CAPES) – Brazil - Finance Code 001. María Artiga-Artigas thanks the University of Lleida for her pre-doctoral fellowship. Laura Salvia-Trujillo thanks the “Secretaria d’Universitats i Recerca del Departament d’Empresa i Coneixement de la Generalitat de Catalunya” for the Beatriu de Pinós post-doctoral grant (BdP2016-00336).

References

Bonnaire, L., Sandra, S., Helgason, T., Decker, E. A., Weiss, J., & McClements, D. J. (2008). Influence of lipid physical state on the in vitro digestibility of emulsified lipids. *Journal of Agricultural and Food Chemistry*, *56*(10), 3791–3797.

Boon, C. S., McClements, D. J., Weiss, J., & Decker, E. A. (2010). Factors Influencing the Chemical Stability of Carotenoids in Foods. *Critical Reviews in Food Science and Nutrition*, *50*(6), 515–532.

569 Guo, Q., Bellissimo, N., & Rousseau, D. (2017). The Physical State of Emulsified
570 Edible Oil Modulates Its in Vitro Digestion. *Journal of Agricultural and Food*
571 *Chemistry*, *65*(41).

572 Guo, Q., Bellissimo, N., & Rousseau, D. (2018). Effect of Emulsifier Concentration and
573 Physical State on the in Vitro Digestion Behavior of Oil-in-Water Emulsions.
574 *Journal of Agricultural and Food Chemistry*, *66*(28), 7496–7503.

575 Hart, S. M., Lin, X. L., Thilakarathna, S. H., & Wright, A. J. (2018). Emulsion droplet
576 crystallinity attenuates early in vitro digestive lipolysis and beta-carotene
577 bioaccessibility. *Food Chemistry*, *260*, 145–151.

578 Levy, E., Goldstein, R., Freier, S., & Shafrir, E. (1981). Characterization of gastric
579 lipolytic activity. *Biochimica et Biophysica Acta (BBA)/Lipids and Lipid*
580 *Metabolism*, *664*(2), 316–326.

581 Liu, W., Wang, J., McClements, D. J., & Zou, L. (2018). Encapsulation of β-carotene-
582 loaded oil droplets in caseinate/alginate microparticles: Enhancement of carotenoid
583 stability and bioaccessibility. *Journal of Functional Foods*, *40*, 527–535.

584 Mehnert, W., & Mäder, K. (2001). Solid lipid nanoparticles: Production,
585 characterization and applications. *Advanced Drug Delivery Reviews*, *47*(2–3), 165–
586 196.

587 Minekus, M., Alminger, M., Alvito, P., Ballance, S., Bohn, T., Bourlieu, C., …
588 Brodkorb, A. (2014). A standardised static in vitro digestion method suitable for
589 food - an international consensus. *Food & Function*, *5*(6), 1113–1124.

590 Muller, R. H., Mader, K., & Gohla, S. (2000). Solid lipid nanoparticles (SLN) for
591 controlled drug delivery - a review of the state of the art. *European Journal of*
592 *Pharmaceutics and Biopharmaceutics*, *50*(1), 161–177.

593 Nik, A M, Langmaid, S., & Wright, A. J. (2012). Digestibility and β-carotene release
594 from lipid nanodispersions depend on dispersed phase crystallinity and interfacial
595 properties. *Food and Function*, *3*(3), 234–245.

596 Nik, Amir Malaki, Langmaid, S., & Wright, A. J. (2012). Nonionic surfactant and
597 interfacial structure impact crystallinity and stability of ??-carotene loaded lipid
598 nanodispersions. *Journal of Agricultural and Food Chemistry*, *60*(16), 4126–4135.

599 Palmero, P., Panozzo, A., Simatupang, D., Hendrickx, M., & Van Loey, A. (2014).
600 Lycopene and beta-carotene transfer to oil and micellar phases during in vitro
601 digestion of tomato and red carrot based-fractions. *Food Research International*,
602 *64*, 831–838.

603 Pascoviche, D. M., Goldstein, N., Fishman, A., & Lesmes, U. (2019). Impact of fatty
604 acids unsaturation on stability and intestinal lipolysis of bioactive lipid droplets.
605 *Colloids and Surfaces A: Physicochemical and Engineering Aspects*, *561*, 70–78.

606 Qian, C., Decker, E. A., Xiao, H., & McClements, D. J. (2013). Impact of lipid
607 nanoparticle physical state on particle aggregation and β-carotene degradation:
608 Potential limitations of solid lipid nanoparticles. *Food Research International*,
609 *52*(1), 342–349.

610 Rao, J., & McClements, D. J. (2011). Food-grade microemulsions, nanoemulsions and
611 emulsions: Fabrication from sucrose monopalmitate & lemon oil. *Food*

Hydrocolloids, *25*(6), 1413–1423.

Rao, A. V, & Rao, L. G. (2007). Carotenoids and human health. *Pharmacological Research*, *55*(3), 207–216.

Salvia-Trujillo, L., Qian, C., Martín-Belloso, O., & McClements, D. J. (2013). Influence of particle size on lipid digestion and beta-carotene bioaccessibility in emulsions and nanoemulsions. *Food Chemistry*, *141*(2), 1475–1480.

Salvia-Trujillo, L., Verkempinck, S. H. E., Sun, L., Van Loey, A. M., Grauwet, T., & Hendrickx, M. E. (2017). Lipid digestion, micelle formation and carotenoid bioaccessibility kinetics: Influence of emulsion droplet size. *Food Chemistry*, *229*, 653–662.

Salvia-Trujillo, L, Qian, C., Martín-Belloso, O., & McClements, D. J. (2013). Modulating β-carotene bioaccessibility by controlling oil composition and concentration in edible nanoemulsions. *Food Chemistry*, *139*(1–4), 878–884. https://doi.org/10.1016/j.foodchem.2013.02.024

Salvia-Trujillo, L, Soliva-Fortuny, R., Rojas-Grau, M. A., McClements, D. J., & Martin-Belloso, O. (2017). Edible Nanoemulsions as Carriers of Active Ingredients: A Review. *Annual Review of Food Science and Technology, Vol 8*, *8*, 439–466.

Salvia-Trujillo, Laura, Rojas-Graü, A., Soliva-Fortuny, R., & Martín-Belloso, O. (2013). Physicochemical characterization of lemongrass essential oil-alginate anoemulsions: effect of ultrasound processing parameters. *Food and Bioprocess Technology*, *6*(9), 2439–2446.

Salvia-Trujillo, Laura, Verkempinck, S., Rijal, S. K., Van Loey, A., Grauwet, T., & Hendrickx, M. (2019a). Lipid nanoparticles with fats or oils containing β-carotene: Storage stability and in vitro digestibility kinetics. *Food Chemistry*, *278*, 396–405.

Salvia-Trujillo, Laura, Verkempinck, S., Rijal, S. K., Van Loey, A., Grauwet, T., & Hendrickx, M. (2019b). Lipid nanoparticles with fats or oils containing β-carotene: Storage stability and in vitro digestibility kinetics. *Food Chemistry*, *278*, 396–405.

Singh, H., Ye, A., & Horne, D. (2009). Structuring food emulsions in the gastrointestinal tract to modify lipid digestion. *Progress in Lipid Research*, *48*(2), 92–100.

Verkempinck, S. H. E., Salvia-Trujillo, L., Moens, L. G., Carrillo, C., Van Loey, A. M., Hendrickx, M. E., & Grauwet, T. (2018). Kinetic approach to study the relation between in vitro lipid digestion and carotenoid bioaccessibility in emulsions with different oil unsaturation degree. *Journal of Functional Foods*, *41*, 135–147.

Verkempinck, S. H. E., Salvia-Trujillo, L., Moens, L. G., Charleer, L., Van Loey, A. M., Hendrickx, M. E., & Grauwet, T. (2018). Emulsion stability during gastrointestinal conditions effects lipid digestion kinetics. *Food Chemistry*, *246*, 179–191.

Verrijssen, T. A., Christiaens, S., Verkempinck, S. H., Boeve, J., Grauwet, T., Van Loey, A. M., … Hendrickx, M. E. (2016). In vitro β-Carotene Bioaccessibility and Lipid Digestion in Emulsions: Influence of Pectin Type and Degree of Methyl-Esterification. *Journal of Food Science*, *81*(10).

Wang, Q., Huang, J., Hu, C., Xia, N., Li, T., & Xia, Q. (2017). Stabilization of a non-aqueous self-double-emulsifying delivery system of rutin by fat crystals and nonionic surfactants: Preparation and bioavailability study. *Food and Function*, *8*(7), 2512–2522.

Weiss, J., Decker, E. A., McClements, D. J., Kristbergsson, K., Helgason, T., & Awad, T. (2008). Solid lipid nanoparticles as delivery systems for bioactive food components. *Food Biophysics*, *3*(2), 146–154.

Witzleb, R., Müllertz, A., Kanikanti, V.-R., Hamann, H.-J., & Kleinebudde, P. (2012). Dissolution of solid lipid extrudates in biorelevant media. *International Journal of Pharmaceutics*, *422*(1–2), 116–124.

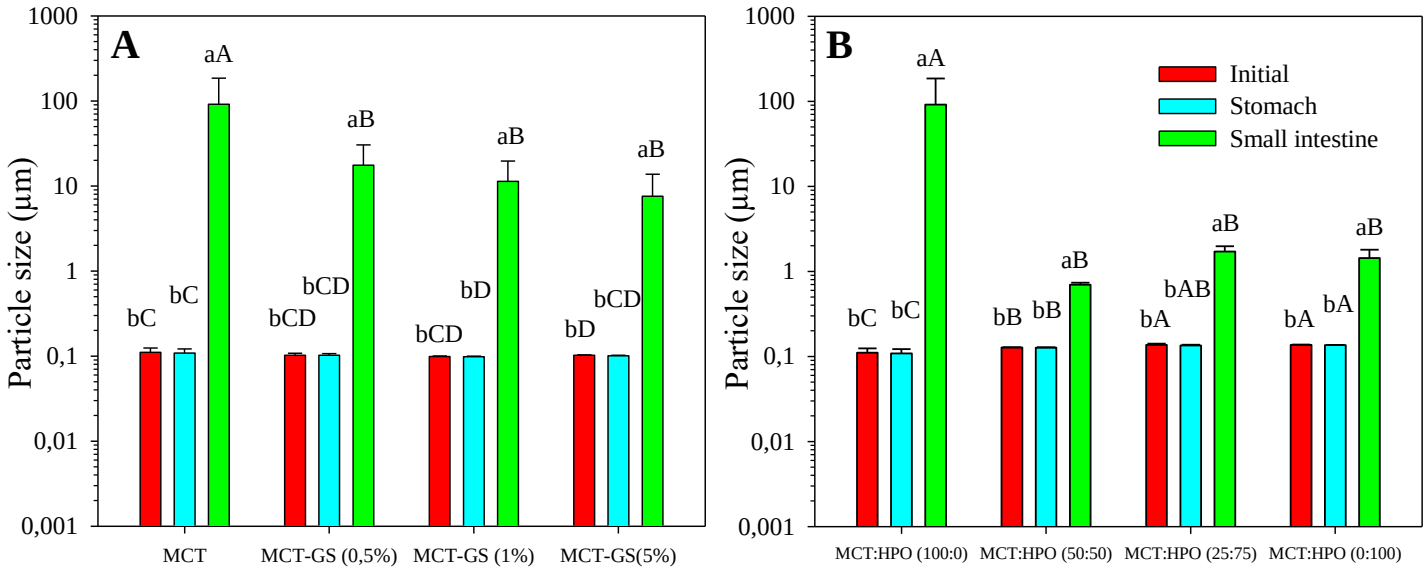

Figure 1. Average particle diameter (µm) of nanoemulsions and solid lipid nanoparticles formulated with different lipid phases consisting on a medium chain tryglyceride (MCT) and glyceryl stearate (GS) at different concentrations (A) or hydrogenated palm oil (HPO) at different ratios (B) initially and after being submitted to simulated gastric and small intestinal conditions.

Different lower case letters indicate significant differences between different GIT phases for the same type of lipid phase. Different upper case letters indicate significant differences between samples for the same GIT phase and different lipid phase.

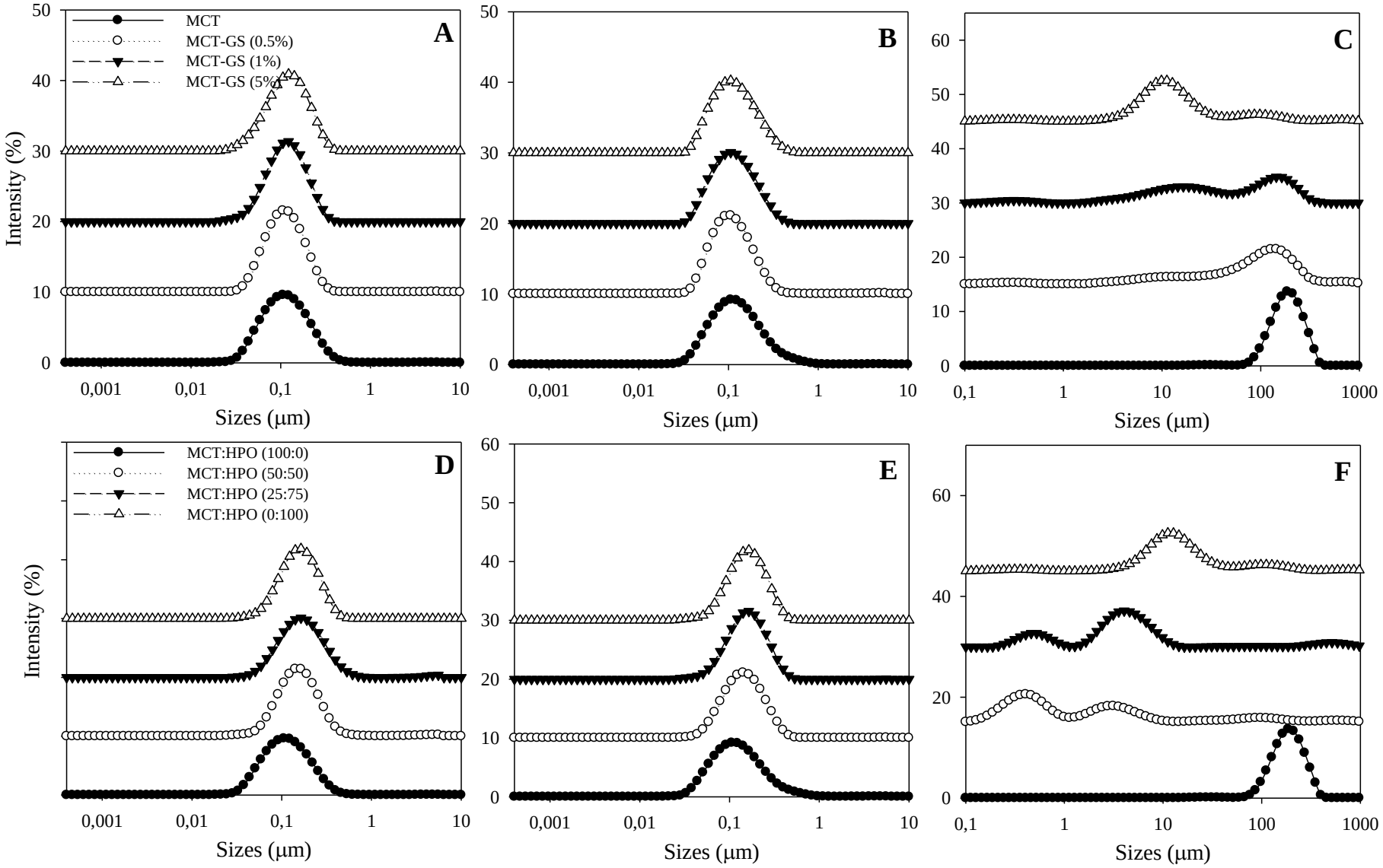

Figure 2. Particle size distribution in intensity (%) of nanoemulsions and solid lipid nanoparticles formulated with different lipid phases consisting on a medium chain tryglyceride (MCT) mixed with glyceryl stearate (GS) at different concentrations (A, B, and C) or with hydrogenated palm oil (HPO) (D, E, F) initially (A, D) and after being submitted to simulated gastric (B, E) and small intestinal conditions (C, F).

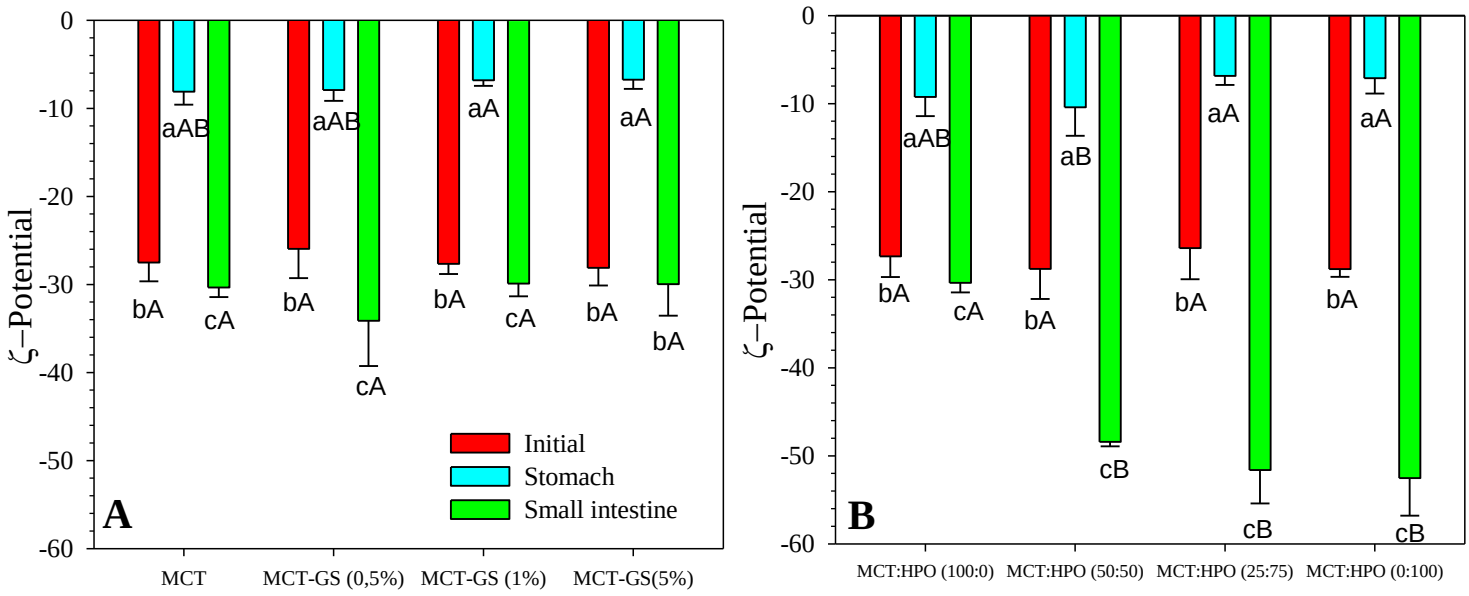

Figure 3. ζ-potential (mV) of nanoemulsions and solid lipid nanoparticles formulated with different lipid phases consisting on a medium chain tryglyceride (MCT) and glyceryl stearate (GS) at different concentrations (A) or hydrogenated palm oil (HPO) at different ratios (B) initially and after being submitted to simulated gastric and small intestinal conditions.

Different lower case letters indicate significant differences between different GIT phases for the same type of lipid phase. Different upper case letters indicate significant differences between samples for the same GIT phase and different lipid phase.

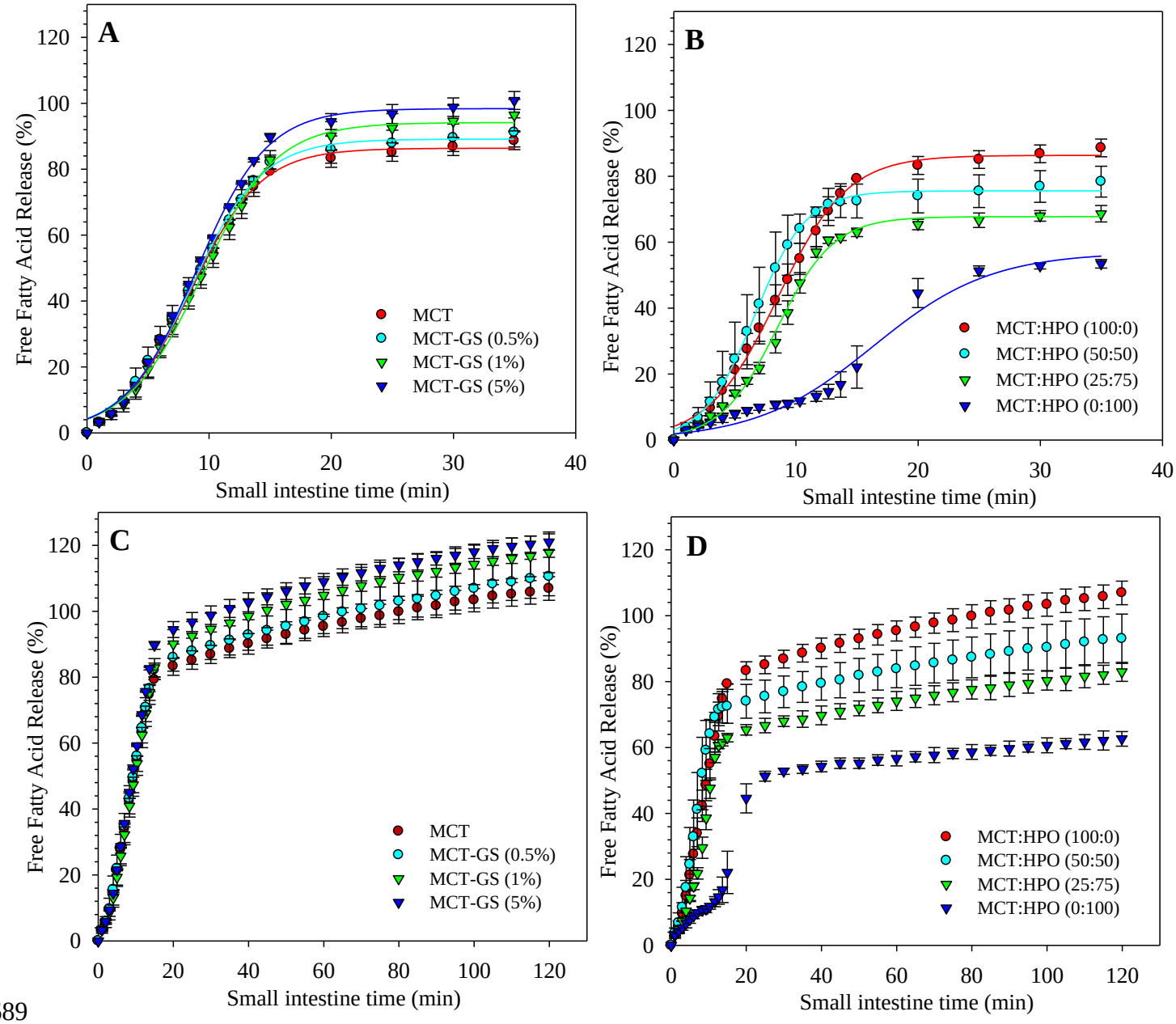

Figure 4. Lipid digestion kinetics expressed as free fatty acid release (%) during small intestinal time (min) of nanoemulsions and solid lipid nanoparticles formulated with different lipid phases consisting on a medium chain tryglyceride (MCT) and glyceryl stearate (GS) at different concentrations (A, C) or hydrogenated palm oil (HPO) at different ratios (B, D). Lipid digestion kinetics up to 35 min of intestinal phase was modelled using a sigmoidal equation and full symbols represent experimental data points and lines are predicted values. Full, dotted, dashed and dotted-dashed lines correspond to MCT, MCT-0.5% GS, MCT-1% GS and MCT-5% GS or MCT:HPO 100:0, 50:50, 25:75 and 0:100.

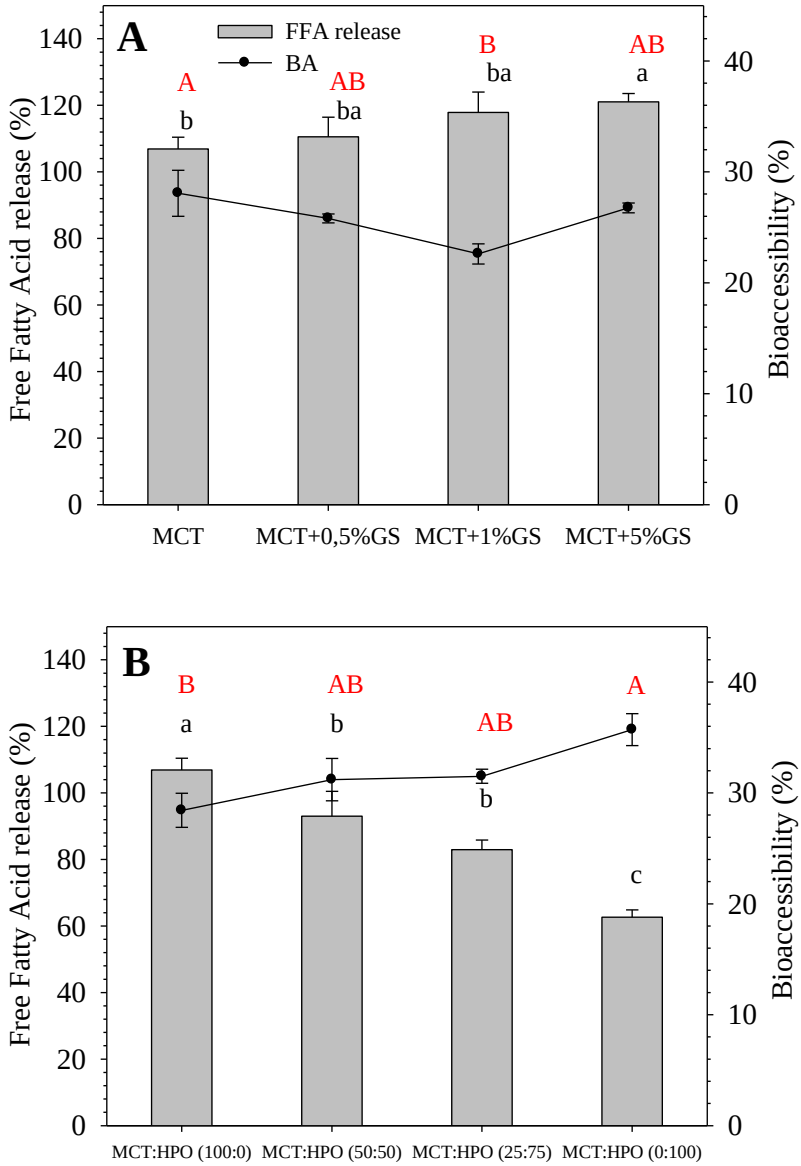

699

700 Figure 5. β-carotene bioaccessibility (%) (lines) in relation of the lipid digestibility in terms of free fatty
701 acid release (%) (bars) at the end of the *in vitro* small intestinal phase (120 min) of nanoemulsions and
702 solid lipid nanoparticles formulated with different lipid phases consisting on a medium chain
703 tryglyceride (MCT) and glyceryl stearate (GS) at different concentrations (A) or hydrogenated palm oil
704 (HPO) at different ratios (B).

705 Lower case letters indicate significant differences between the β-carotene bioaccessibility values while
706 different upper case letters indicate significant differences between the free fatty acid release.

707

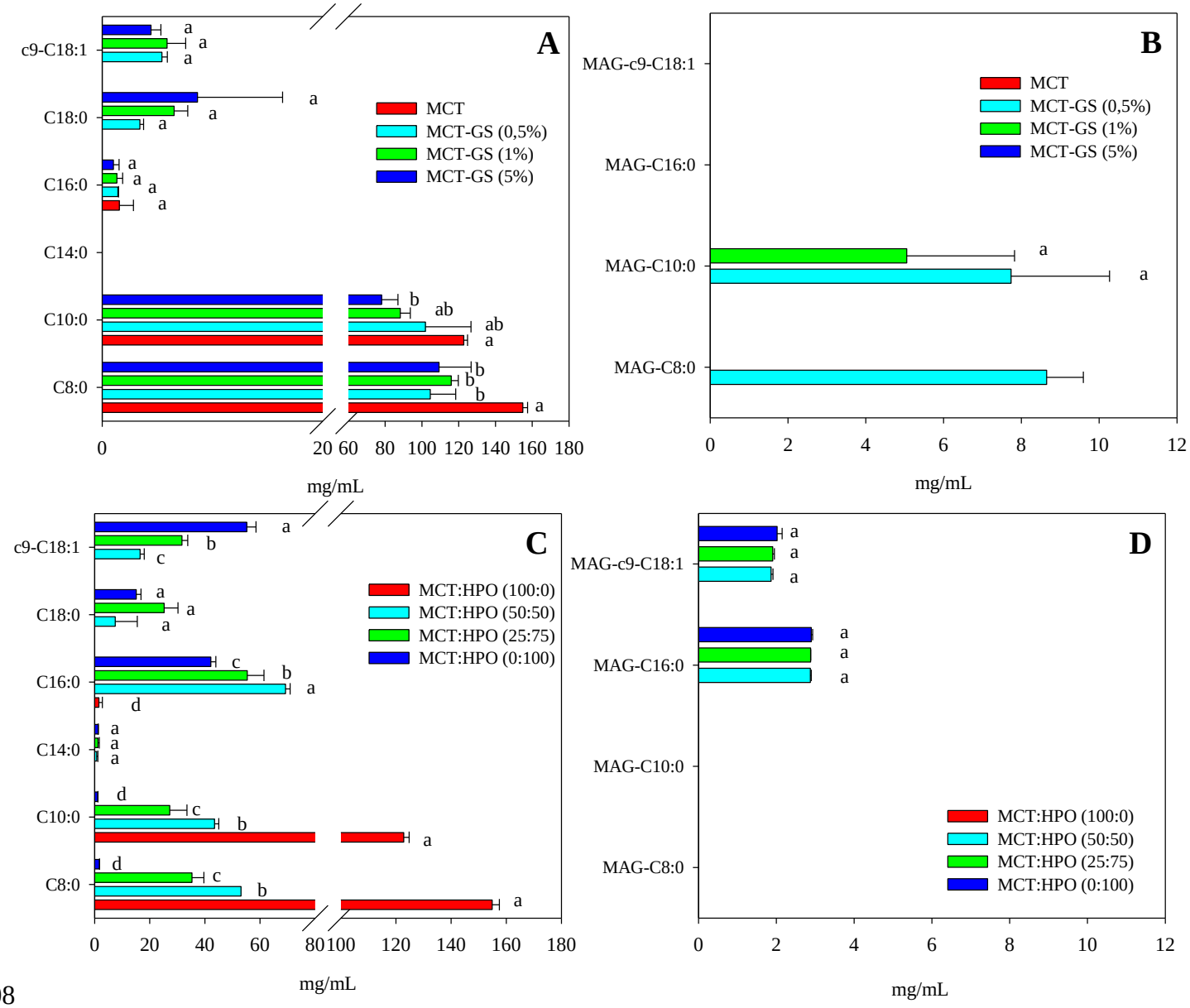

Figure 6. Micelle fraction composition in terms of free fatty acids (A,C) and monoacylglycerides (B, D) of nanoemulsions and solid lipid nanoparticles formulated with different lipid phases consisting on a medium chain tryglyceride (MCT) and glyceryl stearate (GS) at different concentrations (A, B) or hydrogenated palm oil (HPO) at different ratios (C, D).

Lower case letters indicate significant differences within the same lipid species and different lipid phase.

Figure A. Differential scanning calorimetry profiles of the lipid phases used for the formulation of liquid lipid nanoparticles with MCT (A) or solid lipid nanoparticles with MCT blended with glyceryl stearate (GS) at a concentration of 0.5, 1 and 5 % (w/w) (B, C and D, respectively). Upper lines are the cooling cicles and lower lines are the heating cycles. The crystallization (T_c) and melting (T_m) temperatures are provided for each peak and its respective difference of enthalpy (ΔH_f).

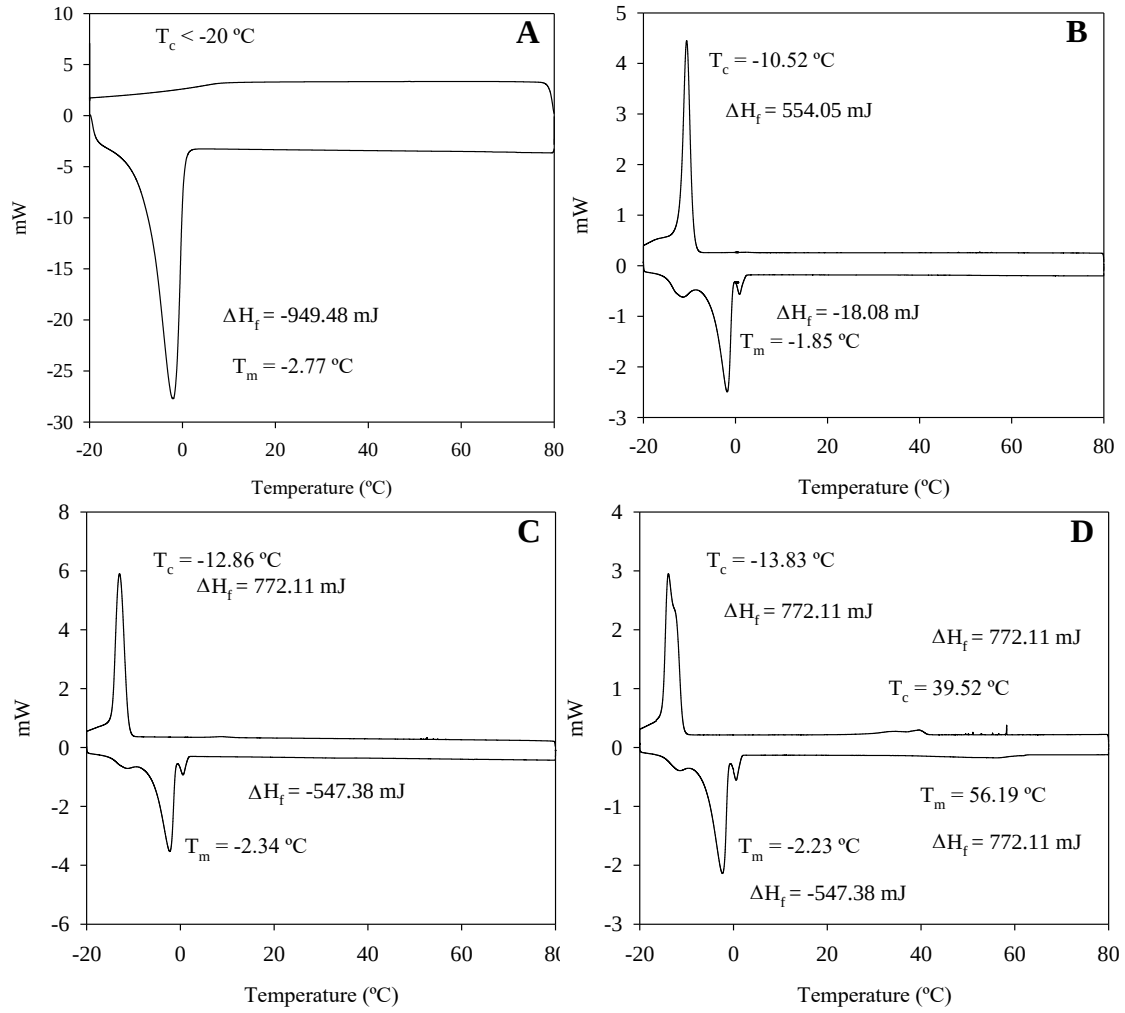

Figure B. Differential scanning calorimetry profiles of the lipid phases used for the formulation of liquid lipid nanoparticles with MCT (A) or solid lipid nanoparticles with MCT blended with hydrogenated palm oil (HPO) at a ratio of 50:50, 25:75 and 0:100 of MCT:HPO (B, C and D, respectively). Upper lines are the cooling cicles and lower lines are the heating cycles. The crystallization (T_c) and melting (T_m) temperatures are provided for each peak and its respective difference of enthalpy (ΔH_f).

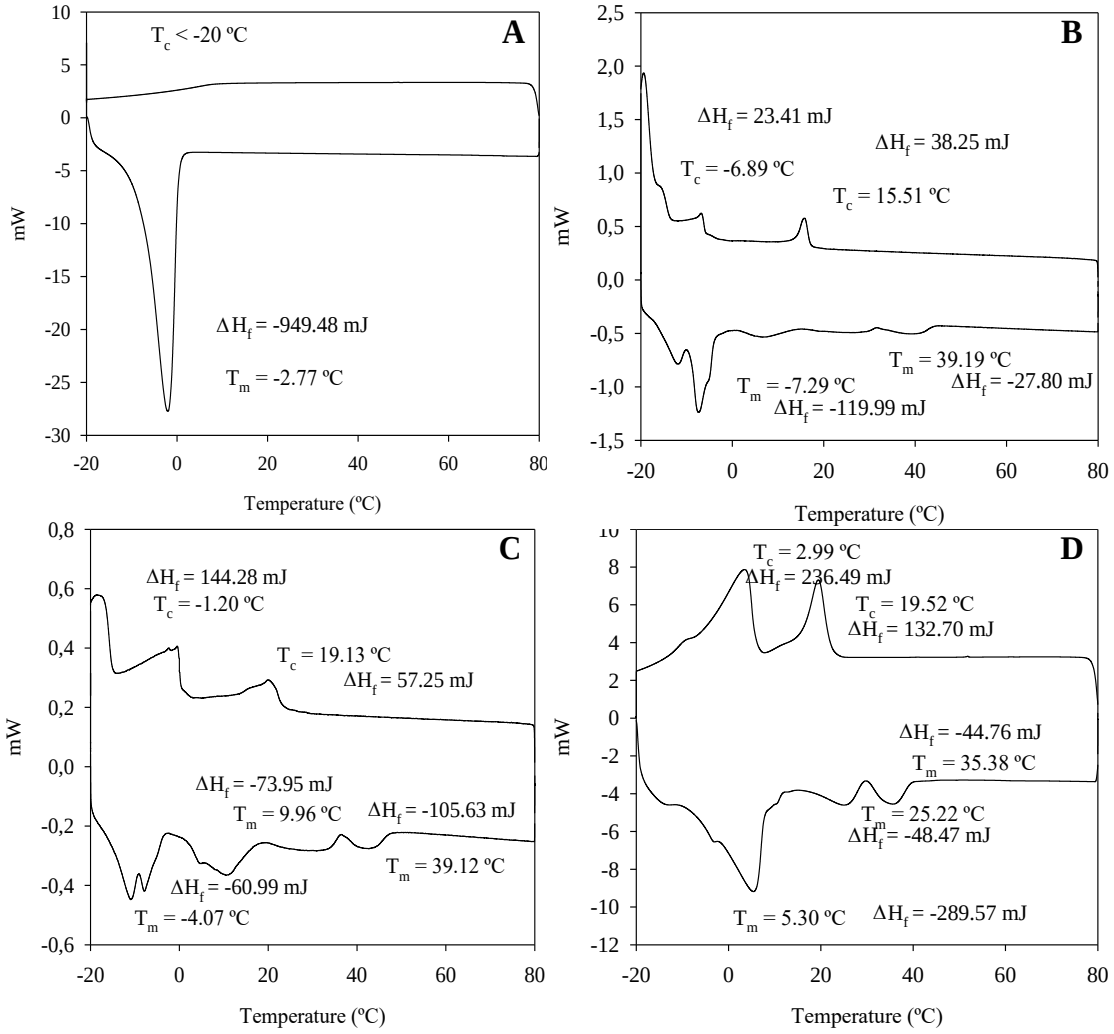

Figure C. Microscopy images of liquid lipid nanoparticles and solid lipid nanoparticles formulated with different lipid phases consisting on a medium chain tryglyceride (MCT) and glyceryl stearate (GS) at different concentrations initially and after being submitted to simulated gastric and small intestinal conditions.

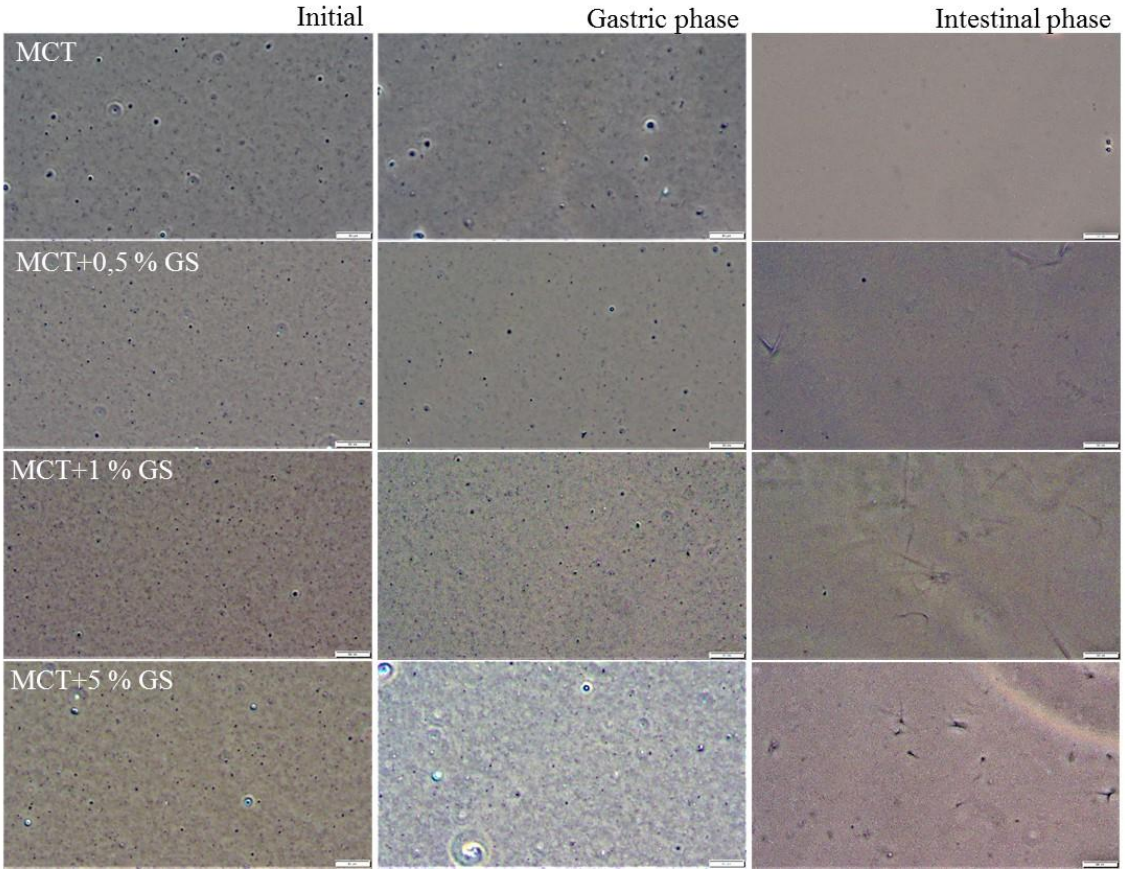

Figure D. Microscopy images of liquid lipid nanoparticles and solid lipid nanoparticles formulated with different lipid phases consisting on a medium chain tryglyceride (MCT) and hydrogenated palm oil (HPO) at different concentrations initially and after being submitted to simulated gastric and small intestinal conditions.

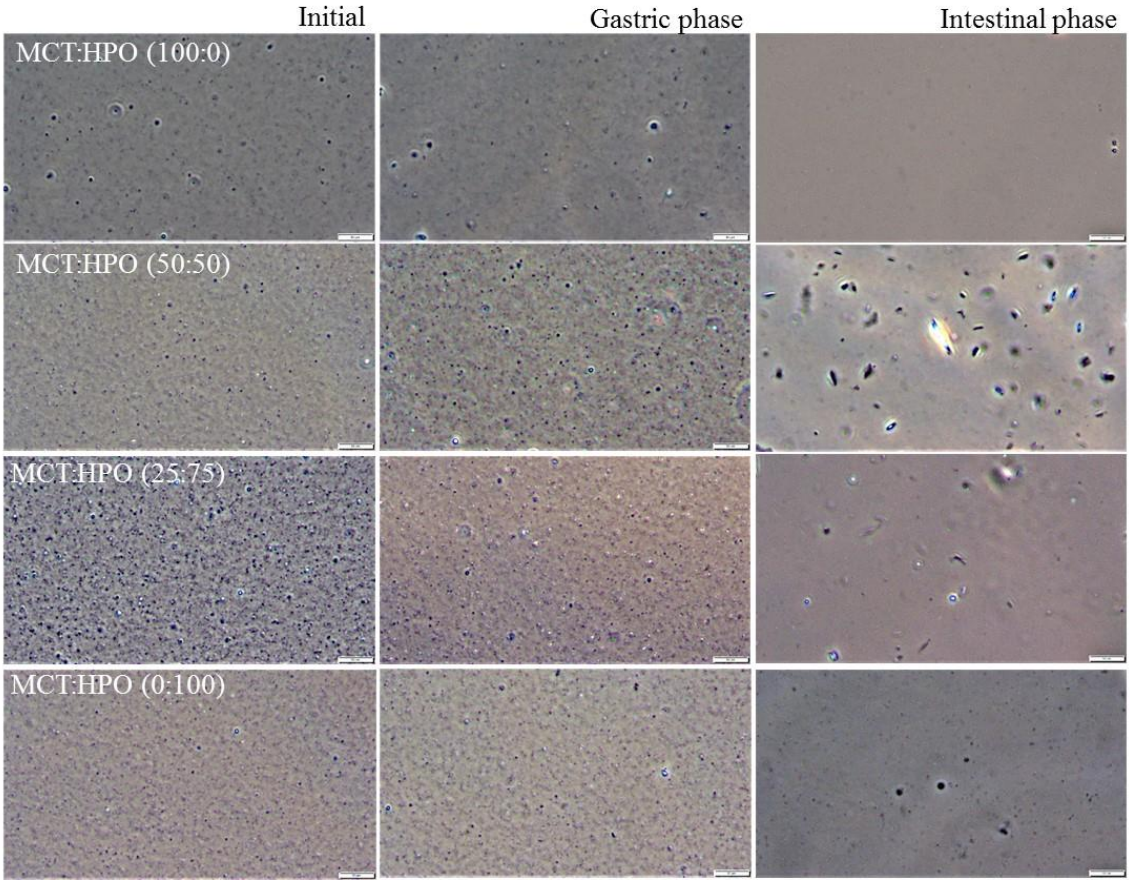

Table A. Estimated kinetic parameters of the logistic model fitted to experimental data of free fatty acid release of liquid or solid lipid nanoparticles formulated with medium chain triglyceride oil (MCT) or MCT containing different concentrations of glyceryl stearate (GS) during the first 35 min of *in vitro* small intestinal phase.

Sample	k	a	b	R^2
MCT	0.351 ± 0.013 [a]	8.515 ± 0.129 [a]	86.34 ± 0.96 [a]	0.997
MCT+GS 0.5 %	0.348 ± 0.013 [a]	8.585 ± 0.136 [a]	89.12 ±1.04 [a]	0.997
MCT+GS 1 %	0.328 ± 0.011 [a]	9.344 ± 0.130 [b]	94.13 ± 1.03 [b]	0.997
MCT+GS 5 %	0.346 ± 0.012 [a]	8.955 ± 0.129 [ab]	98.37 ± 1.09 [c]	0.997

k is the kinetic rate constant, a is the inflexion point of the curve and b is the asymptotic parameter. Different lower case levels indicate statistically significant differences in the same estimated kinetic parameter between the different lipid phases of the lipid nanoparticles.

Table B. Estimated kinetic parameters of the logistic model fitted to experimental data of free fatty acid release of liquid or solid lipid nanoparticles formulated with medium chain triglyceride oil (MCT) or hydrogenated palm oil (HPO) and their blends at different ratios during the first 35 min of *in vitro* small intestinal phase.

Sample	k	a	b	R^2
MCT: HPO (100:0)	0.351 ± 0.013 [b]	8.515 ± 0.129 [b]	86.34 ± 0.96 [d]	0.997
MCT:HPO (50:50)	0.476 ± 0.015 [cc]	6.625 ± 0.079 [a]	75.56 ± 0.55 [c]	0.998
MCT:HPO (25:75)	0.460 ± 0.130 [cc]	8.460 ± 0.130 [b]	67.75 ± 0.83 [b]	0.996
MCT:HPO (0:100)	0.209 ± 0.022 [a]	16.328 ± 0.796 [c]	56.92 ± 2.55 [a]	0.997

k is the kinetic rate constant, a is the inflexion point of the curve and b is the asymptotic parameter. Different lower case levels indicate statistically significant differences in the same estimated kinetic parameter between the different lipid phases of the lipid nanoparticles.